Research Repository UCD

Title	Frequency Participation Factors
Authors(s)	Ortega, Alvaro, Milano, Federico
Publication date	2018-03-05
Publication information	Ortega, Alvaro, and Federico Milano. “Frequency Participation Factors.” IEEE, March 5, 2018. https://doi.org/10.1109/TPWRS.2018.2812423.
Publisher	IEEE
Item record/more information	http://hdl.handle.net/10197/9999
Publisher's statement	© 2018 IEEE. Personal use of this material is permitted. Permission from IEEE must be obtained for all other uses, in any current or future media, including reprinting/republishing this material for advertising or promotional purposes, creating new collective works, for resale or redistribution to servers or lists, or reuse of any copyrighted component of this work in other works.
Publisher's version (DOI)	10.1109/TPWRS.2018.2812423

Downloaded 2026-05-01 23:36:12

The UCD community has made this article openly available. Please share how this access benefits you. Your story matters! (@ucd_oa)

© Some rights reserved. For more information

Frequency Participation Factors

Álvaro Ortega, *Member, IEEE*, Federico Milano, *Fellow, IEEE*

***Abstract*— This paper discusses two quantitative and complementary approaches to evaluate the participation of synchronous generators and interconnection buses on local bus frequency variations during electromechanical transients. Both approaches are based on the concept of *frequency divider formula* recently proposed by the authors on these transactions. A thorough comparison of the two approaches is provided considering several scenarios and three networks, namely the New England 39-bus test system, the all-island 1,479-bus Irish transmission system, and the ENTSO-E 21,177-bus transmission system.**

***Index Terms*— Frequency estimation, frequency measurement, participation factors, synchronous machines, transient stability analysis.**

I. Introduction

A. Motivations

The problem of how to define the participation of generators to losses and transmission rights in transmission systems has been under intense research for more than two decades [1]–[10]. The solution of such a problem is particularly relevant in electricity markets where the costs of the utilization of the network should be shared among all participants. An analogous emerging problem, which has not been investigated so far, is the participation of synchronous machines and nodes at which the frequency is imposed, e.g., interconnection buses, to the frequency variations at network buses. To be able to evaluate such participation is relevant as the high penetration of non-synchronous, often renewable, generation leads to a drastic reduction of the inertia and frequency control of the system [11], [12] and, potentially, to a considerable impact on the variation and rate of change of the frequency [13]–[18]. This paper presents a formal procedure to evaluate frequency participation factors (FPF) and proposes quantitative tools to define how the inertia present in the system influences frequency variations at network buses.

B. Rationale and Literature Review

In order to define FPFs, one has first to be able to estimate how the frequency varies from point to point in the grid. This is actually not a straightforward task, as the conventional power system model for transient stability analysis only retains synchronous machine electro-mechanical equations and neglects frequency variations in transmission lines, transformers and loads.

With this aim, in [19]–[21], the authors have proposed and validated through extensive simulations and comprehensive case studies the *frequency divider* formula that, under some approximations and assumptions, provides an accurate estimation of the frequency variations at every bus of the network by means of a linear combination of the variations of the rotor speeds of all synchronous machines operating in the system.

The frequency divider formula involves a matrix ($\mathbf{D}$, according to the notation utilized in [19]) which, from a formal point of view, is structurally similar to the matrix $\bar{\mathbf{F}}_{LG}$ defined in [22], [23], which gives the percentage participation that each generator has in establishing the no-load voltage at each bus. Both matrices, in fact, are obtained from the partitioning or augmentation of the network admittance matrix $\bar{\mathbf{Y}}_{\mathrm{bus}}$, as originally proposed in [24] in the context of voltage stability analysis. The observation that matrices $\mathbf{D}$ and $\bar{\mathbf{F}}_{LG}$ are formally equivalent leads to the following relevant property, which originates the present work: the elements of each row of $\mathbf{D}$ are the FPF of each synchronous machine rotor speed (or any other device and node at which the frequency is imposed) to the bus frequencies.

In the literature, the concept of *participation factors* has been extensively applied to a variety of electrical quantities. In [10], two analytical expressions, referred to as *power divider laws*, are proposed to define the sensitivities of line current flows to nodal current injections, called *current injection sensitivity factors*. The aim of the power divider laws is to map nodal active- and reactive-power injections to active- and reactive-power flows on the lines of AC transmission networks.

In [25], the authors propose a Model Predictive Control (MPC)-based coordinated control for multi-terminal HVDC grids to ensure power balance in the system while avoiding current and or voltage limit violations, in a time frame of seconds/few minutes. To this aim, [25] considers the concept of *power participation factors* (PPFs) to update the reference powers of the converters of the HVDC systems, being the summation of all PPFs equal to unity.

A MPC-based Automatic Generation Control (AGC) for secondary frequency control of multi-area power systems is proposed in [26]. In the optimization problem, participation factors for all synchronous machines are defined as optimization variables to determine the outputs of the AGC that are distributed to each generator.

Finally, in [27] and [28], the authors propose to evaluate the sensitivities of voltage and reactive power variations based on a partition of the Jacobian matrix of the power flow equations. The *voltage participation factors* (VPFs) proposed in these references are computed based on the right and

Álvaro Ortega and Federico Milano are with the School of Electrical and Electronic Engineering, University College Dublin, Ireland.

E-mails: alvaro.ortegamanjavacas@ucd.ie; federico.milano@ucd.ie

This material is based upon works supported by the European Commission Ireland, by funding Á. Ortega and F. Milano, under the RESERVE Consortium (grant No. 727481). F. Milano is also funded by the Science Foundation Ireland, under Investigator Programme, Grant No. SFI/15/IA/3074, and a beneficiary of the EC Marie Skłodowska-Curie CIG No. PCIG14-GA-2013-630811.

left eigenvectors of the eigenvalues of such reduced Jacobian matrix.

To the best of our knowledge, the concept of *participation factors* applied to bus frequencies as proposed in this paper, has not been yet applied in the literature. The proposed FPFs show relevant differences both conceptually and/or in their applications with respect to the references above, as follows.

First, the FPFs are not based on eigenvalue analysis as opposed to the VPFs presented in [27], [28]. Rather, the FPFs are the components of the linear expressions that relate each bus frequency to the rotor speeds of synchronous machines. Then, the proposed FPFs are a consequence of the topology of the system and machine parameters. Therefore, FPFs cannot be chosen/modified for/by a controller or any other agent such as system operators. This is in contrast with the participation factors described in [25] and [26], as they are chosen based on the capability of each converter to reschedule their power flows, and on the result of an optimal control problem, respectively.

Despite all the aforementioned advantages of matrix $\mathbf{D}$, it nevertheless shows a significant limitation from the practical implementation point of view. As the result of the product of a matrix inverse by another matrix, in fact, $\mathbf{D}$ is generally fully dense, i.e., each bus frequency depends on the rotor speeds of *all* machines. It is to be expected, however, that rotor speeds do not all weight in the same way when calculating the frequency at a given bus. One thus needs an efficient and robust criterion to define which elements of the rows of $\mathbf{D}$ are most relevant for the calculation of bus frequencies without loss of accuracy. To define such a trade-off is the main objective of this paper.

C. Contributions

The contributions of the paper are the following.

- A discussion on the formal equivalence of matrices $\mathbf{D}$ and $\bar{\mathbf{F}}_{LG}$.
- An exhaustive comparison of two approaches proposed to reduce the density of matrix $\mathbf{D}$ while retaining the accuracy of the bus frequency estimation.
- A comprehensive discussion of a proposed method to retain the main advantages of robustness and efficiency of both approaches by means of an appropriate combination.
- A discussion on the practical implications of FPFs.

D. Paper Organization

The remainder of the paper is organized as follows. Section II shows the formal equivalence of matrices $\mathbf{D}$ and $\bar{\mathbf{F}}_{LG}$ and Section III describes the two proposed approaches to define most relevant FPFs and, in turn, reduce the density of matrix $\mathbf{D}$. Section III-C also illustrates the performance of both approaches by means of the New England 39-bus, 10-machine test system. An exhaustive case study is provided in Section IV, that includes a large number of scenarios considering the all-island Irish and the ENTSO-E real-world transmission networks. A discussion of the practical applications of FPFs is included in Section V. Finally, Section VI draws conclusion and future work directions.

II. Background

This section recalls the formulation of the frequency divider formula and its equivalence to the $\bar{\mathbf{F}}_{LG}$ matrix used in [22]–[24].

A. Definition and Properties of the $\bar{\mathbf{F}}_{LG}$ Matrix

The starting point is the well-known network admittance matrix $\bar{\mathbf{Y}}_{\text{bus}}$, which is discussed in many books, e.g., [29]. This matrix is first partitioned into load (L) and generation (G) blocks:

$$\bar{\mathbf{Y}}_{\text{bus}} = \begin{bmatrix} \bar{\mathbf{Y}}_{GG} & \bar{\mathbf{Y}}_{GL} \\ \bar{\mathbf{Y}}_{LG} & \bar{\mathbf{Y}}_{LL} \end{bmatrix} \tag{1}$$

where $\bar{\mathbf{Y}}_{GG} \in \mathbb{C}^{n_G \times n_G}$, $\bar{\mathbf{Y}}_{LL} \in \mathbb{C}^{n_L \times n_L}$; $\bar{\mathbf{Y}}_{GL} \in \mathbb{C}^{n_G \times n_L}$; and $\bar{\mathbf{Y}}_{LG} \in \mathbb{C}^{n_L \times n_G}$. In this context, load buses are all buses where there is no generation. Transition buses are thus assumed to be load buses with zero consumption. If there are no phase shifting transformers in the grid, then $\bar{\mathbf{Y}}_{\text{bus}}$ is symmetrical and, hence, $\bar{\mathbf{Y}}_{GL} = \bar{\mathbf{Y}}_{LG}^T$.

The $\bar{\mathbf{F}}_{LG}$ matrix is defined as:

$$\bar{\mathbf{F}}_{LG} = -\bar{\mathbf{Y}}_{LL}^{-1}\bar{\mathbf{Y}}_{LG} \tag{2}$$

which has the following properties: (i) its elements are almost real-valued; and (ii) its rows sum close to unity. While these properties have been noticed and exploited in various works, e.g., [30], [31], it has been only recently, that formal proofs of such properties have been found [32]. Note that, if $\bar{\mathbf{Y}}_{LL}$ is singular, i.e., no shunt elements are present, $\bar{\mathbf{F}}_{LG}$ can be still defined using the Moore-Penrose pseudo-inverse of $\bar{\mathbf{Y}}_{LL}$.

B. Definition and Properties of the $\mathbf{D}$ Matrix

The frequency divider formula as proposed in [19] is based on the augmented admittance matrix that is obtained including the nodes of the emfs (denoted with subscript E) behind the impedances of the synchronous machines:

$$\begin{bmatrix} \bar{\mathbf{Y}}_{EE} & \bar{\mathbf{Y}}_{EB} \\ \bar{\mathbf{Y}}_{BE} & \bar{\mathbf{Y}}_{\text{bus}} + \bar{\mathbf{Y}}_{E0} \end{bmatrix} \tag{3}$$

where $\bar{\mathbf{Y}}_{EE} \in \mathbb{C}^{n_G \times n_G}$, $\bar{\mathbf{Y}}_{E0} \in \mathbb{C}^{n_B \times n_B}$; $\bar{\mathbf{Y}}_{EB} \in \mathbb{C}^{n_G \times n_B}$; and $\bar{\mathbf{Y}}_{BE} \in \mathbb{C}^{n_B \times n_G}$, with $n_B = n_G + n_L$ being the total number of buses. Matrix $\bar{\mathbf{Y}}_{E0}$ is a diagonal matrix that accounts for the internal impedances of the synchronous machines at generator buses. Matrix $\bar{\mathbf{Y}}_{EE}$ is diagonal and its elements are the inverse of the internal impedances of the synchronous machines connected at buses G. Finally, $\bar{\mathbf{Y}}_{EB} = \bar{\mathbf{Y}}_{BE}^T$ always holds.

According to the notation of (3), the frequency divider formula is given by:

$$\Delta\boldsymbol{\omega}_B = \mathbf{D}\Delta\boldsymbol{\omega}_G \tag{4}$$

with:

$$\mathbf{D} = -\left(\text{Im}\{\bar{\mathbf{Y}}_{\text{bus}} + \bar{\mathbf{Y}}_{E0}\}\right)^{-1} \text{Im}\{\bar{\mathbf{Y}}_{BE}\} \tag{5}$$

where $\Delta\boldsymbol{\omega}_B$ are the estimated frequency variations at system buses and $\Delta\boldsymbol{\omega}_G$ are synchronous machine rotor speed variations. Matrix $\text{Im}\{\bar{\mathbf{Y}}_{\text{bus}} + \bar{\mathbf{Y}}_{E0}\}$ is full rank if $\text{Im}\{\bar{\mathbf{Y}}_{E0}\} \neq \mathbf{0}$, which is always satisfied in practice.

We observe that all hypotheses that are assumed in Theorem 2.1 in [32] and that apply to (1) and (2) also apply to (3) and (5), respectively. This leads to the conclusion that $\bar{\mathbf{F}}_{LG}$ and $\mathbf{D}$ can be shown to have same properties and, hence, the rows of $\mathbf{D}$ sum close to 1. Moreover, $\mathbf{D}$ is real by definition, hence we do not need that the R/X ratio is the same for every network branch, which is the condition to have a real $\mathbf{F}_{LG}$ (see Proposition 2.1 in [32]).

It is relevant to note that the quantities forming the vector $\boldsymbol{\omega}_G$ do not need to be obtained from synchronous machines. Boundary buses that define the interconnections with external grids or buses at which the frequency is controlled by large non-synchronous generators can be used in (4), provided that accurate frequency measures are available at those buses, e.g., by means of phasor measurement unit (PMU) devices. In these cases, the elements of the matrices $\bar{\mathbf{Y}}_{BE}$ and $\bar{\mathbf{Y}}_{E0}$ are the inverse of the Thevenin equivalent impedances of such external networks. The interested reader can find more details in [19]. In the remainder of the paper, without loss of generality, we will assume that $\boldsymbol{\omega}_G$ consists of synchronous machine rotor speed measurements.

III. Proposed Approaches to Define Relevant FPFs

This section presents the two approaches proposed in this paper to reduce the density of the frequency divider matrix $\mathbf{D}$ while retaining the accuracy of bus frequency estimation. The aim of this density reduction is to define the most relevant FPFs. The features of each approach are duly discussed.

Let $\sigma_{\mathrm{D},i}$ be the summation of the elements of the i-th row of $\mathbf{D}$. As stated in the previous subsection, the following applies:

$$\sigma_{\mathrm{D},i} = \sum_{j=1}^{n_G} D_{i,j} \approx 1, \quad \forall i = 1, \ldots, n_B \tag{6}$$

Each element $D_{i,j}$ of the frequency divider matrix $\mathbf{D}$ thus represents the FPF – or normalized weight – of the synchronous machine rotor speed or the frequency measurement $\omega_{G,j}$ to the frequency of bus $\omega_{B,i}$.

As anticipated in the introduction, matrix $\mathbf{D}$ is dense as it is obtained from the product of two matrices, one of which is the inverse of the imaginary part of the admittance matrix, as shown in (5). Even though the admittance matrix is very sparse, in fact, the inverse is generally fully dense. Hence, the FPFs $D_{i,j}$ tends to be all non-zero.

Let d_D be the density index of matrix $\mathbf{D}$, such that:

$$d_D = 100 \cdot \frac{n_{\mathrm{NNZ}}}{(n_G \cdot n_B)} \tag{7}$$

where n_{NNZ} is the number of non-zero elements of $\mathbf{D}$. According to the discussion above, one has, in general, $d_D \approx 100\%$. For large networks, however, one would expect that generators that are geographically (and electrically) far away from a given bus, do not significantly participate to the frequency of that bus. This intuition is confirmed by the observation that, at least in large networks, a large number of elements of $\mathbf{D}$ are *small*. To quantify how small an element has to be such that it can be safely neglected without compromising the accuracy of the estimation of bus frequencies, however, is not a trivial task. In the following subsections, we propose two complementary approaches to tackle this problem.

A. Approach 1 (A1)

In this approach, the elements of each row i of $\mathbf{D}$ are sorted in descending order according to their magnitudes. Then, the first, and thus the biggest m_i elements of each row of the sorted matrix $\tilde{\mathbf{D}}$ are summed such that:

$$\sum_{h=1}^{m_i} \tilde{D}_{i,h} < \alpha_{\mathrm{D}} \sigma_{\mathrm{D},i} \tag{8}$$

where $\alpha_{\mathrm{D}} \in [0, 1]$ is a given threshold. Finally, the reduced matrix $\mathbf{D}_{\mathrm{r}}$ is obtained by setting to zero all elements $\tilde{D}_{i,h^*}$ with $h^* = m_i + 1, \ldots, n_B$, and rearranging $\tilde{D}_{i,h \cup h^*}$ according to their original positions before the sorting, i.e., $D_{i,j}$. Therefore, if $\alpha_{\mathrm{D}} \to 0$, the number of elements of $\tilde{\mathbf{D}}$, and thus of $\mathbf{D}$, that are neglected increases. Limits cases are as follows:

$$\mathbf{D}_{\mathrm{r}} = \begin{cases} \mathbf{0}\ , & \text{if } \alpha_{\mathrm{D}} = 0\ ; \\ \mathbf{D}\ , & \text{if } \alpha_{\mathrm{D}} = 1\ . \end{cases} \tag{9}$$

Hence, the closer α_{D} is to 0, the sparser and less accurate is the matrix $\mathbf{D}_{\mathrm{r}}$.

The main advantage of this approach is that it guarantees at least the specified accuracy of the frequency estimation at every bus. However, the sorting of $\tilde{\mathbf{D}}$, and the evaluation of (8) must be done for each row, thus leading to a high computational burden for large networks.

B. Approach 2 (A2)

The reduced matrix $\mathbf{D}_{\mathrm{r}}$ is obtained by neglecting all the elements of $\mathbf{D}$ that are below a threshold, as follows:

$$D_{\mathrm{r}i,j} = \begin{cases} 0\ , & \text{if } D_{i,j} < \epsilon_{\mathrm{D}} \cdot \max(\mathbf{D}); \\ D_{i,j}, & \text{otherwise.} \end{cases} \tag{10}$$

where $\max(\mathbf{D})$ is the maximum value of the elements in $\mathbf{D}$, and $\epsilon_{\mathrm{D}} \in [0, 1]$ is a given parameter and, generally, $\epsilon_{\mathrm{D}} \ll 1$.

While this approach is considerably simpler and computationally more efficient than the previous one, it lacks the capability to control the desired accuracy of the estimated bus frequencies as provided by A1. In fact, if the FPFs of $\boldsymbol{\omega}_G$ to the frequency of the i-th bus are similar, and if ϵ_{D} is too high, there would be the risk of neglecting several relevant measures. On the other hand, if ϵ_{D} is too low, all FPFs and thus also non-meaningful ones would be taken into account. Therefore, a careful, network-based tuning of ϵ_{D} is required.

C. Illustrative Example

In this section, the features of the two approaches A1 and A2 proposed above are illustrated by means of the well-known New England 39-bus, 10-machine test system [33].

Results are shown in Tables I and II, respectively. Considering $\alpha_{\mathrm{D}} = 0.6$ and $\epsilon_{\mathrm{D}} = 0.123$, the density of $\mathbf{D}_{\mathrm{r}}$, $d_{\mathrm{D_r}}$, is the same for both approaches, and equal to 34.62%. It can be seen that, despite achieving the same $d_{\mathrm{D_r}}$ in both cases, matrix $\mathbf{D}_{\mathrm{r}}$ is substantially different. Note that using A1, the values of the normalized summations of the rows of $\mathbf{D}_{\mathrm{r}}$ over their respective rows of $\mathbf{D}$, i.e., $\sigma_{\mathrm{D_{r}}i}/\sigma_{\mathrm{D}_i}$, are more uniformly distributed than those using A2. While the minimum $\sigma_{\mathrm{D_{r}}i}/\sigma_{\mathrm{D}_i}$ obtained using

TABLE I: Matrix $\mathbf{D}_{\mathrm{r}}$ of the 39-bus test system using A1. $\alpha_{\mathrm{D}} = 0.6$; $d_{\mathrm{D_r}} = 34.62\%$.

	Generator											
Bus	1	2	3	4	5	6	7	8	9	10	σ_{D_i}	$\frac{\sigma_{\mathrm{D}_{\mathrm{r}i}}}{\sigma_{\mathrm{D}_i}}$
1	0	0	0	0	0	0	0	0	0	0.67	1.109	0.604
2	0.3	0	0	0	0	0	0	0.093	0	0.358	1.152	0.652
3	0.236	0	0.085	0	0	0	0	0	0.09	0.35	1.171	0.65
4	0.182	0.098	0.118	0	0	0	0	0	0	0.378	1.171	0.662
5	0.159	0.117	0.126	0	0	0	0	0	0	0.41	1.165	0.697
6	0.157	0.122	0.129	0	0	0	0	0	0	0.407	1.164	0.7
7	0.152	0	0.122	0	0	0	0	0	0	0.436	1.162	0.612
8	0.15	0	0.118	0	0	0	0	0	0	0.451	1.16	0.62
9	0	0	0	0	0	0	0	0	0	0.693	1.115	0.622
10	0.158	0.106	0.162	0	0	0	0	0	0	0.373	1.167	0.685
11	0.158	0.111	0.151	0	0	0	0	0	0	0.385	1.167	0.689
12	0.161	0.108	0.152	0	0	0	0	0	0	0.38	1.175	0.682
13	0.162	0.103	0.152	0	0	0	0	0	0	0.371	1.17	0.674
14	0.172	0.095	0.129	0	0	0	0	0	0	0.362	1.175	0.645
15	0.174	0	0	0.111	0	0.118	0	0	0	0.313	1.181	0.606
16	0.174	0	0	0.123	0	0.13	0	0	0	0.291	1.181	0.608
17	0.197	0	0	0	0	0.111	0	0	0.109	0.308	1.186	0.612
18	0.212	0	0	0	0	0.101	0	0	0.102	0.325	1.182	0.626
19	0.152	0	0	0.205	0	0.113	0	0	0	0.255	1.17	0.62
20	0.139	0	0	0.187	0.109	0	0	0	0	0.233	1.101	0.607
21	0.162	0	0	0	0	0.167	0.13	0	0	0.271	1.176	0.621
22	0.149	0	0	0	0	0.205	0.153	0	0	0.249	1.167	0.649
23	0.148	0	0	0	0	0.184	0.177	0	0	0.248	1.166	0.65
24	0.171	0	0	0.12	0	0.138	0	0	0	0.286	1.18	0.605
25	0.263	0	0	0	0	0	0	0.14	0	0.326	1.166	0.625
26	0.219	0	0	0	0	0	0	0.102	0.194	0.302	1.208	0.676
27	0.209	0	0	0	0	0.097	0	0	0.155	0.306	1.201	0.639
28	0.196	0	0	0	0	0	0	0	0.309	0.27	1.216	0.637
29	0.187	0	0	0	0	0	0	0	0.344	0.258	1.209	0.652
30	0.481	0	0	0	0	0	0	0	0	0.256	1.091	0.675
31	0.128	0.224	0	0	0	0	0	0	0	0.333	1.077	0.636
32	0.13	0	0.254	0	0	0	0	0	0	0.307	1.08	0.639
33	0.13	0	0	0.261	0	0.097	0	0	0	0.218	1.086	0.65
34	0.132	0	0	0.177	0.149	0	0	0	0	0.22	1.087	0.623
35	0.133	0	0	0	0	0.272	0.136	0	0	0.222	1.126	0.677
36	0.128	0	0	0	0	0.159	0.29	0	0	0.214	1.143	0.692
37	0.226	0	0	0	0	0	0	0.241	0	0.279	1.121	0.666
38	0.163	0	0	0	0	0	0	0	0.406	0.225	1.161	0.684
39	0	0	0	0	0	0	0	0	0	0.846	1.062	0.796

TABLE II: Matrix $\mathbf{D}_{\mathrm{r}}$ of the 39-bus test system using A2. $\epsilon_{\mathrm{D}} = 0.123$; $\max(\mathbf{D}) = 0.846$; $d_{\mathrm{D_r}} = 34.62\%$.

	Generator											
Bus	1	2	3	4	5	6	7	8	9	10	σ_{D_i}	$\frac{\sigma_{\mathrm{D}_{\mathrm{r}i}}}{\sigma_{\mathrm{D}_i}}$
1	0.155	0	0	0	0	0	0	0	0	0.67	1.109	0.743
2	0.3	0	0	0	0	0	0	0	0	0.358	1.152	0.571
3	0.236	0	0	0	0	0	0	0	0	0.35	1.171	0.501
4	0.182	0	0.118	0	0	0	0	0	0	0.378	1.171	0.579
5	0.159	0.117	0.126	0	0	0	0	0	0	0.41	1.165	0.697
6	0.157	0.122	0.129	0	0	0	0	0	0	0.407	1.164	0.7
7	0.152	0.115	0.122	0	0	0	0	0	0	0.436	1.162	0.711
8	0.15	0.111	0.118	0	0	0	0	0	0	0.451	1.16	0.716
9	0	0	0	0	0	0	0	0	0	0.693	1.115	0.622
10	0.158	0.106	0.162	0	0	0	0	0	0	0.373	1.167	0.685
11	0.158	0.111	0.151	0	0	0	0	0	0	0.385	1.167	0.689
12	0.161	0.108	0.152	0	0	0	0	0	0	0.38	1.175	0.682
13	0.162	0	0.152	0	0	0	0	0	0	0.371	1.17	0.585
14	0.172	0	0.129	0	0	0	0	0	0	0.362	1.175	0.564
15	0.174	0	0	0.111	0	0.118	0	0	0	0.313	1.181	0.606
16	0.174	0	0	0.123	0	0.13	0.107	0	0	0.291	1.181	0.699
17	0.197	0	0	0.105	0	0.111	0	0	0.109	0.308	1.186	0.701
18	0.212	0	0	0	0	0	0	0	0	0.325	1.182	0.454
19	0.152	0	0	0.205	0	0.113	0	0	0	0.255	1.17	0.62
20	0.139	0	0	0.187	0.109	0	0	0	0	0.233	1.101	0.607
21	0.162	0	0	0.114	0	0.167	0.13	0	0	0.271	1.176	0.718
22	0.149	0	0	0.105	0	0.205	0.153	0	0	0.249	1.167	0.739
23	0.148	0	0	0.105	0	0.184	0.177	0	0	0.248	1.166	0.74
24	0.171	0	0	0.12	0	0.138	0.117	0	0	0.286	1.18	0.705
25	0.263	0	0	0	0	0	0	0.14	0.114	0.326	1.166	0.723
26	0.219	0	0	0	0	0	0	0	0.194	0.302	1.208	0.592
27	0.209	0	0	0	0	0	0	0	0.155	0.306	1.201	0.558
28	0.196	0	0	0	0	0	0	0	0.309	0.27	1.216	0.637
29	0.187	0	0	0	0	0	0	0	0.344	0.258	1.209	0.652
30	0.481	0	0	0	0	0	0	0	0	0.256	1.091	0.675
31	0.128	0.224	0.106	0	0	0	0	0	0	0.333	1.077	0.735
32	0.13	0	0.254	0	0	0	0	0	0	0.307	1.08	0.639
33	0.13	0	0	0.261	0	0	0	0	0	0.218	1.086	0.561
34	0.132	0	0	0.177	0.149	0	0	0	0	0.22	1.087	0.623
35	0.133	0	0	0	0	0.272	0.136	0	0	0.222	1.126	0.677
36	0.128	0	0	0	0	0.159	0.29	0	0	0.214	1.143	0.692
37	0.226	0	0	0	0	0	0	0.241	0	0.279	1.121	0.666
38	0.163	0	0	0	0	0	0	0	0.406	0.225	1.161	0.684
39	0	0	0	0	0	0	0	0	0	0.846	1.062	0.796

A1 is 0.604 at bus 1 highlighted in light gray in Table I, one can find 9 buses with equal or lower $\sigma_{\mathrm{D}_{\mathrm{r}i}}/\sigma_{\mathrm{D}_i}$ in Table II, namely 2, 3, 4, 13, 14, 18, 26, 27, and 33. In fact, in buses 3 ($\sigma_{\mathrm{D}_{\mathrm{r}3}}/\sigma_{\mathrm{D}_3} = 0.501$) and 18 ($\sigma_{\mathrm{D}_{\mathrm{r}18}}/\sigma_{\mathrm{D}_{18}} = 0.454$), these values are 17.1% and 24.8% lower than 0.604, respectively. On the other hand, while only 2 buses have a $\sigma_{\mathrm{D}_{\mathrm{r}i}}/\sigma_{\mathrm{D}_i} \geq 0.7$ using A1, highlighted in dark gray in Table I, this number increases to 12 in the case of A2. This means that, using A1, one can estimate not only the frequency at a given bus, but also the accuracy of such a signal. On the other hand, A2 leads to a higher uncertainty of the accuracy of the estimated signal with respect to the full matrix $\mathbf{D}$.

IV. Case Studies

In this section, two real-world systems are considered, namely, a 1,479-bus model of the all-island Irish transmission system; and a 21,177-bus model of the ENTSO-E transmission system. These systems are used to compare the accuracy and computational efficiency of the two proposed approaches to define the most relevant FPFs, namely A1 and A2. The topology and the steady-state data of both systems are based on the actual real-world systems provided by and the Irish TSO, EirGrid, and ENTSO-E,[1] respectively. However, dynamic data are guessed based on the knowledge of the technology of power plants.

All simulations and plots presented in this section were obtained using the software tool Dome [34] running on a 4 core 2.60 GHz Intel© Core i7™ with 8 GB of RAM.

A. Irish Transmission System

This subsection considers a dynamic model of the all-island Irish transmission system. This includes 1,479 buses, 1,851 transmission lines and transformers, 245 loads, 22 conventional synchronous power plants modeled with 6th order synchronous machine models with AVRs and turbine governors, 6 PSSs and 176 wind power plants, of which 34 are equipped with constant-speed (CSWT) and 142 with doubly-fed induction generators (DFIG).

1) Sensitivity Analysis: Figure 1 shows the density $d_{\mathrm{D_r}}$ of matrix $\mathbf{D}_{\mathrm{r}}$ using A1 and A2 for a range of values of α_{D} and ϵ_{D}, respectively, with increments of 0.01.

Figure **??** shows a saturation at $\alpha_{\mathrm{D}} \approx 0.7$, from which $d_{\mathrm{D_r}}$ increases faster with α_{D}. This indicates that the FPFs of the synchronous machine rotor speeds of the system have a similar weight, due to the short electrical distances between the generation buses with the rest of the grid that characterize the Irish system. Thus, one must take into consideration a high number of elements of $\mathbf{D}$ in order to obtain a good accuracy

[1]ENTSO-E system data have been licensed to the second author by ENTSO-E. Data can be requested through an on-line application at `www.entsoe.eu`.

TABLE III: FPFs of the generators of the Irish system to the bus frequencies. Top: A1 ($\alpha_{\mathrm{D}} = 0.75$). Bottom: A2 ($\epsilon_{\mathrm{D}} = 0.04$).

Generator Bus	715	699	682	857	989	953	987	988	1283	756	992	1221	505	1220	993	1353	1174	1011	1013	1143	1010	1012
Number of Participations	1468	1459	1432	1256	1224	1214	888	746	534	513	457	455	422	342	316	218	160	29	29	18	5	5
Average FPF	0.086	0.066	0.155	0.085	0.057	0.061	0.05	0.054	0.038	0.055	0.064	0.034	0.049	0.033	0.07	0.044	0.024	0.052	0.052	0.163	0.14	0.14

Generator Bus	715	682	699	857	989	953	987	988	756	992	505	993	1283	1221	1220	1353	1010	1011	1012	1013	1174	1143
Number of Participations	1234	1231	1228	1177	1170	1154	1140	1104	717	548	533	526	442	288	181	102	82	82	82	82	21	18
Average FPF	0.099	0.178	0.075	0.089	0.064	0.063	0.049	0.049	0.05	0.059	0.046	0.057	0.041	0.038	0.049	0.068	0.038	0.038	0.038	0.038	0.079	0.163

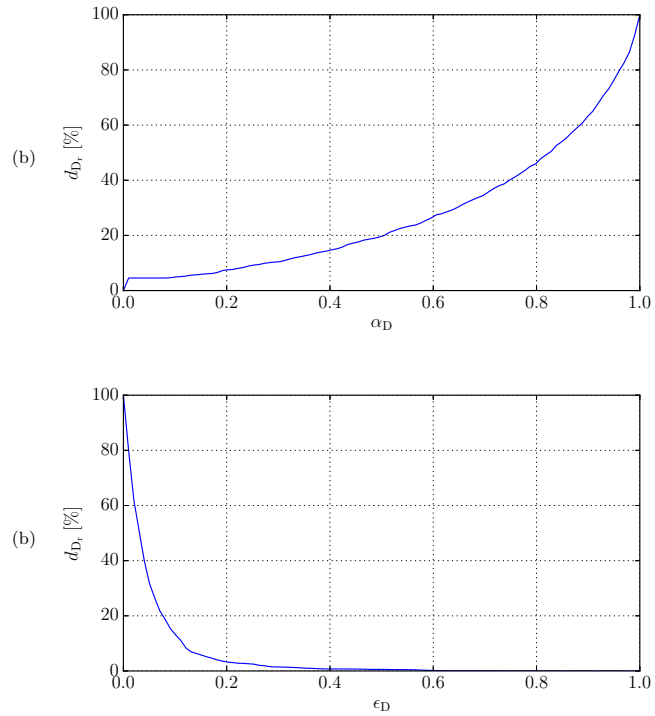

Fig. 1: Density of matrix $\mathbf{D}_{\mathrm{r}}$ of the Irish transmission system. (a) A1; $\alpha_{\mathrm{D}} \in [0, 1]$. (b) A2; $\epsilon_{\mathrm{D}} \in [0, 1]$.

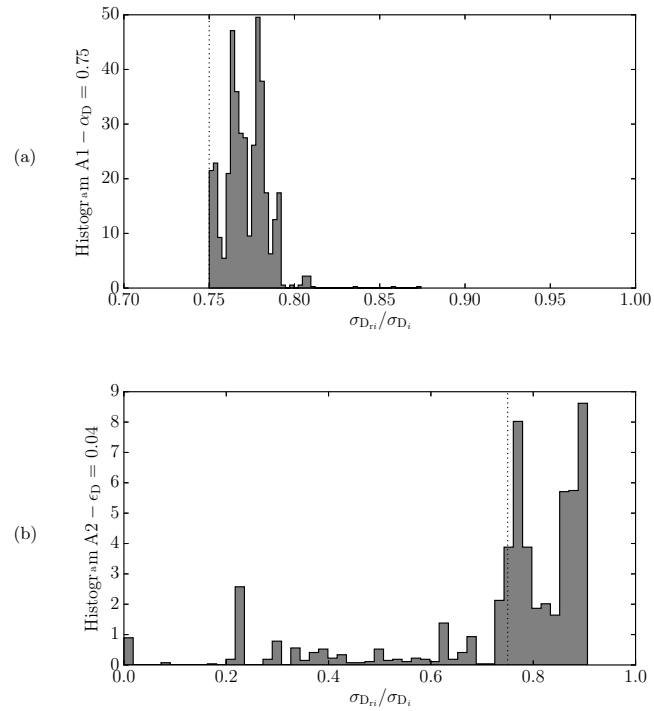

Fig. 2: Histograms of the normalized summations of the FPFs of the Irish transmission system for $d_{\mathrm{D_r}} \simeq 40.5\%$. (a) A1; $\alpha_{\mathrm{D}} = 0.75$. (b) A2; $\epsilon_{\mathrm{D}} = 0.04$.

from $\mathbf{D}_{\mathrm{r}}$. On the other hand, Fig. **??** shows a stiff saturation for $\epsilon_{\mathrm{D}} \in [0, 0.1]$. This indicates that the value of most elements of $\mathbf{D}$ are very small and of similar magnitude.

2) Evaluation of FPFs*:* Subsection III-C illustrates the fact that, for similar densities $d_{\mathrm{D_r}}$, A2 shows a higher variance of the normalized summations of the FPFs, $\sigma_{\mathrm{D_{ri}}}/\sigma_{\mathrm{D_i}}$, than A1. This is shown in Fig. 2, where the histograms of $\sigma_{\mathrm{D_{ri}}}/\sigma_{\mathrm{D_i}}$ for all buses of the Irish system using A1 (Fig. **??**) and A2 (Fig. **??**) are depicted. The chosen values of α_{D} and ϵ_{D} are 0.75 and 0.04, which imply densities of 40.5% and 40.4%, respectively.

Figure **??** shows that, using A1, $\sigma_{\mathrm{D_{ri}}}/\sigma_{\mathrm{D_i}}$ is always greater than $\alpha_{\mathrm{D}} = 0.75$ (marked with a vertical dotted line), and that the number of buses with values greater than 0.8 is very small. Using A2, such a distribution is more spread, and a large number of buses have $\sigma_{\mathrm{D_{ri}}}/\sigma_{\mathrm{D_i}}$ lower than 0.75 or higher than 0.8. Moreover, some buses have $\sigma_{\mathrm{D_{ri}}}/\sigma_{\mathrm{D_i}} = 0$, meaning that all FPFs of the $\boldsymbol{\omega}_G$ at such buses are very similar and of small value, and have been neglected in the computation of $\mathbf{D}_{\mathrm{r}}$, leaving a null row in the matrix.

3) Most Significant Measures: When using the dense matrix $\mathbf{D}$, from the mathematical point of view, all $\boldsymbol{\omega}_G$'s are *needed* in the estimation of the frequency variations at system buses, in the sense that all of them contribute to every $\boldsymbol{\omega}_{B,i}$ in some measure. However, the reduced matrix $\mathbf{D}_{\mathrm{r}}$ allows determining which elements of $\boldsymbol{\omega}_G$ are most significant for the frequency estimation. To this aim, for a given α_{D} or ϵ_{D}, one can determine the number of times a certain $\boldsymbol{\omega}_{G,j}$ contributes in matrix $\mathbf{D}_{\mathrm{r}}$, and/or its average FPF. This is shown in Table III, where the number of FPFs, and their average values, are listed when using A1 ($\alpha_{\mathrm{D}} = 0.75$) and A2 ($\epsilon_{\mathrm{D}} = 0.04$).

The columns of Table III have been sorted in descending order according to the total number of non-null FPFs of each generator in $\mathbf{D}_{\mathrm{r}}$. The 6 generators with the highest average value have been highlighted in gray (the darker, the higher).

An important remark from Table III is that the most relevant generators are those located in buses 682, 715, 857, 699, 989 and 953, regardless of the approach used. This indicates that, from the practical point of view, it is important to have an

accurate and reliable measure of at least the rotor speeds of these machines, or of the frequency variations at these generator buses recorded with PMUs.

4) Dynamic Analysis: In this subsection, the accuracy of matrix $\mathbf{D}_\mathrm{r}$ computed using A1 and A2 for different values of α_D and ϵ_D is studied by means of time domain simulations (TDSs). To this aim, a three-phase fault is simulated at $t = 0.5$ s, and cleared after 250 ms by disconnecting the line.

Figure **??** shows the frequency estimated at a bus where a wind power plant is installed, for different values of α_D, and their respective densities $d_{\mathrm{D_r}}$. The absolute errors ϵ_ω between the trajectories and the ideal case, i.e., using the full matrix $\mathbf{D}$, are depicted in Fig. **??**. The frequency of the center of inertia, ω_COI, is also included as a limit case for the desired accuracy of $\mathbf{D}_\mathrm{r}$. It can be seen that, while the density of matrix $\mathbf{D}_\mathrm{r}$ can be reduced considerably with the A1, it nevertheless captures the local frequency oscillations with a high level of accuracy. Note that, in any case considered, the reduced frequency divider formula outperforms the accuracy of the ω_COI widely-used in these type of studies.

A similar analysis has been performed using A2, and results are shown in Fig. **??**. The values of ϵ_D have been chosen such that the respective densities $d_{\mathrm{D_r}}$ are similar to the A1 scenario. In this case, a better accuracy of the estimation of the frequency at the bus is obtained for equivalent $d_{\mathrm{D_r}}$. However, if other buses are to be analysed, one must take into account the uncertainty that characterizes the accuracy of A2 discussed in Section III-C.

5) Computational Efficiency: The last analysis carried out in the Irish system concerns the computational burden of the two proposed approaches. The CPU times required to initialize the full set of differential algebraic equations (DAEs), and to complete the TDSs of the scenarios described in Subsection IV-A.4 above, are listed in Table IV. The initialization of the full set of DAEs includes the computation of the power flow analysis, and of the reduced matrix $\mathbf{D}_\mathrm{r}$. The implicit trapezoidal method is used for the time integration, with a time step of 0.01 s, and each integration step is solved with the dishonest Newton-Raphson method [29].

TABLE IV: Computational times in seconds of the two approaches studied. Left: A1. Right: A2.

α_D	Init. of full DAEs	TDS
0.95	0.1355	4.0445
0.9	0.1222	3.8408
0.8	0.1157	3.6970
0.6	0.1031	3.5750

ϵ_D	Init. of full DAEs	TDS
0.012	0.1103	3.8216
0.02	0.1037	3.6604
0.035	0.0851	3.4736
0.06	0.0832	3.3643

It can be seen that A2 is slightly more efficient than A1. Both approaches show a similar sensitivity to the density reduction, being considerably faster for lower $d_{\mathrm{D_r}}$. This is also reflected in the TDSs, since matrix $\mathbf{D}_\mathrm{r}$ needs to be computed twice during the simulation (one at the initialization, and another one after the line disconnection due to the change in the system topology).

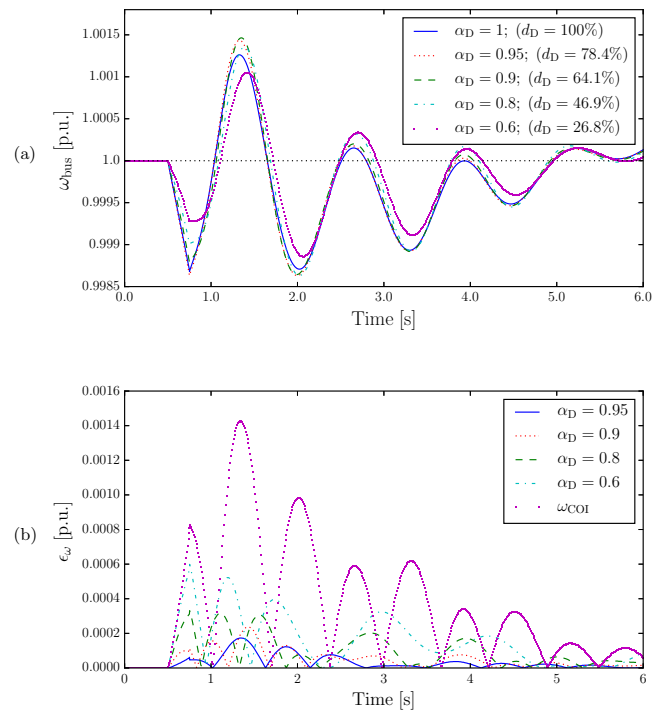

Fig. 3: Frequency estimated at a non-synchronous generation bus of the Irish system facing a three-phase fault using A1. (a) Trajectories. (b) Error.

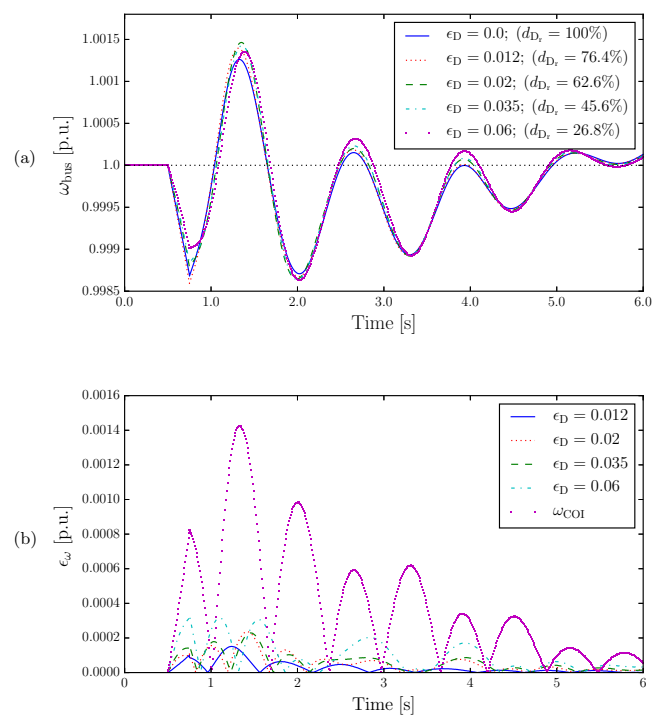

Fig. 4: Frequency estimated at a non-synchronous generation bus of the Irish system facing a three-phase fault using A2. (a) Trajectories. (b) Error.

B. ENTSO-E Transmission System

This subsection considers a dynamic model of the ENTSO-E transmission system. The model includes 21,177 buses (1,212 off-line); 30,968 transmission lines and transformers (2,352 off-line); 1,144 coupling devices, i.e., zero-

impedance connections (420 off-line); 15,756 loads (364 off-line); and 4,832 power plants. Of these power plants, 1,160 are off-line. The system also includes 364 PSSs.

The size of matrix $\mathbf{D}$, including the off-line buses and power plants, is thus (21,177×4,832), with a density $d_{\mathrm{D}} = 84.21\%$. This means that, on average, the estimation of the frequency variations of each bus depend on more than 4,000 power plants with synchronous machines. From the practical point of view, it is clearly not realistic to assume such a dependency, and the need of a reduction of matrix $\mathbf{D}$ density becomes apparent.

To demonstrate that one does not require to retrieve the information of such a large number of generator rotor speeds to estimate the frequency variations at a certain bus, a sensitivity analysis of the ENTSO-E system similar to the one performed in Subsection IV-A.1 is carried out, and results are shown in Fig. 5. In this case, the depicted intervals $\alpha_{\mathrm{D}} \in [0.8, 1]$ and $\epsilon_{\mathrm{D}} \in [0, 0.01]$ have been split into 50 segments with logarithmic increments in order to better capture saturation.

The curves show very stiff saturations, confirming the intuition that the only a small number of generator rotor speeds have significant weights (from Fig. **??**), and that a very high percentage of these weights are extremely small (from Fig. **??**).

In order to ensure a minimum $\sigma_{\mathrm{D}_{\mathrm{r}i}}/\sigma_{\mathrm{D}_i}$ of, e.g., 0.75 using A1 (i.e., $\alpha_{\mathrm{D}} = 0.75$), it is required a density $d_{\mathrm{D}_{\mathrm{r}}} = 1.48\%$. However, the time needed to initialize the set of DAEs (including the computation of matrix $\mathbf{D}_{\mathrm{r}}$) using A1 is 37.021 s. On the other hand, this time is reduced to 8.123 s when using A2 to obtain the same $d_{\mathrm{D}_{\mathrm{r}}}$ ($\epsilon_{\mathrm{D}} = 0.0042$). As opposed to using A1, the minimum $\sigma_{\mathrm{D}_{\mathrm{r}i}}/\sigma_{\mathrm{D}_i}$ of 0.75 can not be guaranteed using A2, and a significant number of buses are below this threshold as shown in Fig. 6.

Therefore, one must choose a trade-off between two crucial aspects such as accuracy and speed of computation. To solve this issue, A1 and A2 can be combined to take advantage of the accuracy achieved with the former, and the computational efficiency of the latter. Combining A1 and A2 consists of the following steps. A2 is firstly applied with a relatively low ϵ_{D}. The aim is to reduce considerably $d_{\mathrm{D}_{\mathrm{r}}}$ without implying a relevant impact on the accuracy of the estimations, as observed from Fig. 5. In this way, the computational burden of the sorting and calculation of (8) can be considerably reduced. Finally, A1 can be then applied with the desired α_{D}.

The effectiveness of the combined approach is considered below. A2 is applied first with $\epsilon_{\mathrm{D}} = 0.0007$ and $d_{\mathrm{D}_{\mathrm{r}}}$ is reduced from the initial 84.21% to 4.45%. As expected, the accuracy has not been deteriorated significantly, as shown in Fig. 7, where all $\sigma_{\mathrm{D}_{\mathrm{r}i}}/\sigma_{\mathrm{D}_i}$ are above 0.9. A1 is then applied with $\alpha_{\mathrm{D}} = 0.75$, with a resulting $d_{\mathrm{D}_{\mathrm{r}}} = 1.48\%$ and with a similar distribution of $\sigma_{\mathrm{D}_{\mathrm{r}i}}/\sigma_{\mathrm{D}_i}$ to the one shown in Fig. **??**. However, the computational time required to initialize the set of DAEs has been reduced from 37.021 s to 18.772 s.

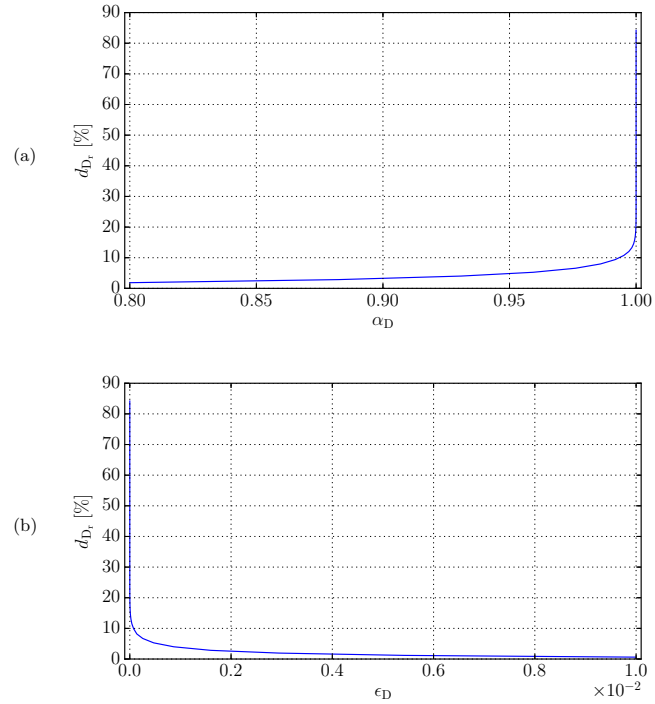

Fig. 5: Density of matrix $\mathbf{D}_{\mathrm{r}}$ of the ENTSO-E transmission system. (a) A1; $\alpha_{\mathrm{D}} \in [0.8, 1]$. (b) A2; $\epsilon_{\mathrm{D}} \in [0, 0.01]$.

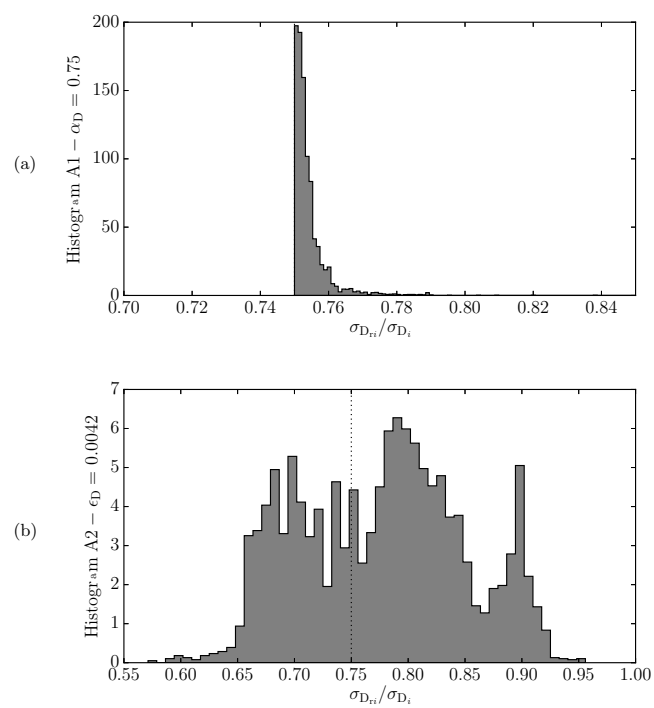

Fig. 6: Histograms of the normalized summations of the FPFs of the ENTSO-E transmission system for $d_{\mathrm{D}_{\mathrm{r}}} = 1.48\%$. (a) A1; $\alpha_{\mathrm{D}} = 0.75$. (b) A2; $\epsilon_{\mathrm{D}} = 0.0042$.

C. Discussion of Results

Based on the results presented in Section IV, the following remarks on the proposed approaches are relevant.

i. Only A1 guarantees the desired accuracy of the frequency estimation at every bus of the network. This is particularly relevant for applications such as dynamic and/or real-time studies, control design, etc.

ii. The applicability of A2 becomes evident in studies that involve very large systems such as the ENTSO-E, due to the simplicity and computational efficiency of this approach.

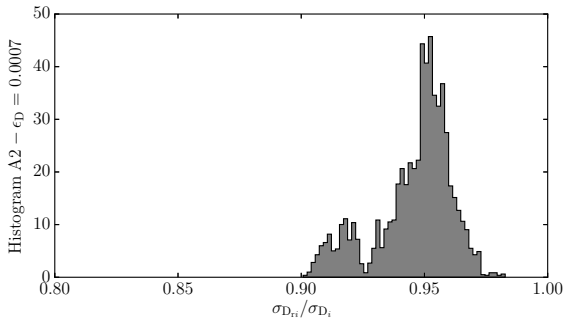

Fig. 7: Histogram of the normalized summations of the FPFs of the ENTSO-E transmission system using A2.

iii. Both A1 and A2 provide similar information about the subset of generators and/or PMU measurements that mostly participate to estimate local frequencies.

iv. A trade-off between computational efficiency and accuracy can be obtained when combining both approaches. The combination can allow carrying out dynamic/real-time studies considering very large systems.

V. Final Remarks on the FPFs

In Section IV, it has been demonstrated that one does not need to take into account of the fully dense $\mathbf{D}$ matrix, but only a very reduced number of elements of such a matrix, to accurately estimate the frequency at every bus of the network in the event of a severe contingency.

The assumption that every bus frequency depends on all synchronous machines, while mathematically correct, is far from convenient in practice, specially if large networks are to be studied. In this vein, Section IV also demonstrates that one can find the most relevant FPFs of every bus frequency signal accurately and efficiently by means of an appropriate combination the two approaches presented in the paper, namely A1 and A2. As a result, this combination allows the application of the proposed FPFs even for very large, real-world networks such as the ENTSO-E transmission system.

It is also important to remark that the study of the system FPFs is only relevant in the time frame of transient stability analysis (i.e., up to few tens of seconds after a large disturbance), as all local bus frequencies will tend to the synchronous frequency after such a time frame (if no instabilities occur).

In particular, accurately defining these FPFs has a significant impact on the following areas.

- *Frequency Stability and Control*: analogously to the techniques aimed at improving voltage stability that are based on bus VPFs, e.g., [22]–[24], [30], [31], FPFs can be used to determine the buses that are most significant for frequency control, e.g., pilot buses as those defined for voltage control (see, for example, [35] and, more recently, [36]).

  FPFs can be also utilized for sensitivity analysis, similarly to the participation factors proposed in [27], to determine which rotor speed mostly affect bus frequency deviations. In fact, differentiating the frequency divider formula (4), one obtains:
  $$\frac{\partial \omega_{B,i}}{\partial \omega_{G,j}} = D_{i,j} \ , \tag{11}$$
  i.e., the sensitivity of the frequency at bus i with respect to the rotor speed of machine j is given by the element (i, j) of matrix $\mathbf{D}$.

  Note that, despite the aforementioned analogies between VPFs and FPFs, the applications of both types of participation factors lie in significantly different time frames: up to tens of minutes for the former, and up to few seconds for the latter. In fact, FPFs can be particularly relevant for, e.g., Rate of Change of Frequency (RoCoF) evaluation, fast frequency control of non-synchronous generation, and identification of weak areas of the system in terms of inertial response of synchronous machines.
- *Frequency State Estimation*: FPFs are useful to design a redundant set of measurements to guarantee a proper system frequency estimation in the event of, e.g., malfunctioning of PMU devices, saturation of the communication system, etc.

VI. Conclusions

The paper discusses two quantitative approaches to evaluate the participation of generators and interconnection buses to the estimation of bus frequencies. These FPFs are relevant for several practical applications, such as the definition of weak areas, from the point of view of the frequency regulation, of the network and frequency state estimation.

The case studies prove the intuition that, in real-world transmission systems, only a reduced number of generators contribute to the frequency of a given bus of the network. Results based on the ENTSO-E system also show that combining the two proposed approaches together leads to an accurate and computationally efficient method.

Future work will focus on the definition of suitable control schemes and state estimation techniques based on FPFs.

References

[1] D. Kirschen, R. Allan, and G. Strbac, "Contributions of individual generators to loads and flows," *IEEE Trans. on Power Systems*, vol. 12, no. 1, pp. 52–60, Feb 1997.

[2] J. Bialek, "Allocation of transmission supplementary charge to real and reactive loads," *IEEE Trans. on Power Systems*, vol. 13, no. 3, pp. 749–754, Aug 1998.

[3] J. Pan, Y. Teklu, S. Rahman, and K. Jun, "Review of usage-based transmission cost allocation methods under open access," *IEEE Trans. on Power Systems*, vol. 15, no. 4, pp. 1218–1224, Nov 2000.

[4] A. Fradi, S. Brignone, and B. E. Wollenberg, "Calculation of energy transaction allocation factors," *IEEE Trans. on Power Systems*, vol. 16, no. 2, pp. 266–272, May 2001.

[5] A. J. Conejo, F. D. Galiana, and I. Kockar, "Z-bus loss allocation," *IEEE Trans. on Power Systems*, vol. 16, no. 1, pp. 105–110, Feb 2001.

[6] P. M. Costa and M. A. Matos, "Loss allocation in distribution networks with embedded generation," *IEEE Trans. on Power Systems*, vol. 19, no. 1, pp. 384–389, Feb 2004.

[7] Q. Ding and A. Abur, "Transmission loss allocation based on a new quadratic loss expression," *IEEE Trans. on Power Systems*, vol. 21, no. 3, pp. 1227–1233, Aug 2006.

[8] A. J. Conejo, J. Contreras, D. A. Lima, and A. Padilha-Feltrin, "Zbus transmission network cost allocation," *IEEE Trans. on Power Systems*, vol. 22, no. 1, pp. 342–349, Feb 2007.

[9] A. M. L. da Silva, J. G. de Carvalho Costa, and L. H. Lopes Lima, "A new methodology for cost allocation of transmission systems in interconnected energy markets," *IEEE Trans. on Power Systems*, vol. 28, no. 2, pp. 740–748, May 2013.
[10] Y. C. Chen and S. V. Dhople, "Power divider," *IEEE Trans. on Power Systems*, vol. 31, no. 6, pp. 5135–5143, Nov 2016.
[11] A. Ulbig, T. S. Borsche, and G. Andersson, "Impact of low rotational inertia on power system stability and operation," in *Procs of the 19th IFAC World Conf.*, vol. 47, no. 3, pp. 7290–7297, Aug 2014.
[12] P. Tielens and D. V. Hertem, "The relevance of inertia in power systems," *Renewable and Sustainable Energy Reviews*, vol. 55, pp. 999–1009, 2016.
[13] M. V. A. Nunes, J. A. P. Lopes, H. H. Zurn, U. H. Bezerra, and R. G. Almeida, "Influence of the variable-speed wind generators in transient stability margin of the conventional generators integrated in electrical grids," *IEEE Trans. on Energy Conversion*, vol. 19, no. 4, pp. 692–701, Dec 2004.
[14] Y. Wang, G. Delille, H. Bayem, X. Guillaud, and B. Francois, "High wind power penetration in isolated power systems – assessment of wind inertial and primary frequency responses," *IEEE Trans. on Power Systems*, vol. 28, no. 3, pp. 2412–2420, Aug 2013.
[15] J. C. M. Vieira, W. Freitas, W. Xu, and A. Morelato, "Efficient coordination of rocof and frequency relays for distributed generation protection by using the application region," *IEEE Trans. on Power Delivery*, vol. 21, no. 4, pp. 1878–1884, Oct 2006.
[16] B. Tamimi, C. Cañizares, and K. Bhattacharya, "System stability impact of large-scale and distributed solar photovoltaic generation: The case of ontario, canada," *IEEE Trans. on Sustainable Energy*, vol. 4, no. 3, pp. 680–688, July 2013.
[17] S. Eftekharnejad, V. Vittal, G. T. Heydt, B. Keel, and J. Loehr, "Impact of increased penetration of photovoltaic generation on power systems," *IEEE Trans. on Power Systems*, vol. 28, no. 2, pp. 893–901, May 2013.
[18] M. Cheng, S. S. Sami, and J. Wu, "Benefits of using virtual energy storage system for power system frequency response," *Applied Energy*, vol. 194, pp. 376–385, 2017.
[19] F. Milano and Á. Ortega, "Frequency divider," *IEEE Trans. on Power Systems*, vol. 32, no. 2, pp. 1493–1501, March 2017.
[20] Á. Ortega and F. Milano, "Comparison of bus frequency estimators for power system transient stability analysis," in *Procs of the POWERCON Conf.*, Wollongong, Australia, Sep 2016, pp. 1–6.
[21] ——, "Impact of frequency estimation for vsc-based devices with primary frequency control," in *Procs of the ISGT Europe Conf.*, Torino, Italy, pp. 1–6, Sep 2017.
[22] D. Thukaram and C. Vyjayanthi, "Relative electrical distance concept for evaluation of network reactive power and loss contributions in a deregulated system," *IET Generation, Transmission Distribution*, vol. 3, no. 11, pp. 1000–1019, Nov 2009.
[23] S. M. Abdelkader, D. J. Morrow, and A. J. Conejo, "Network usage determination using a transformer analogy," *IET Generation, Transmission Distribution*, vol. 8, no. 1, pp. 81–90, Jan 2014.
[24] P. Kessel and H. Glavitsch, "Estimating the voltage stability of a power system," *IEEE Trans. on Power Delivery*, vol. 1, no. 3, pp. 346–354, July 1986.
[25] L. Papangelis, M. S. Debry, P. Panciatici, and T. V. Cutsem, "Coordinated supervisory control of multi-terminal HVDC grids: A model predictive control approach," *IEEE Trans. on Power Systems*, vol. 32, no. 6, pp. 4673–4683, Nov 2017.
[26] A. M. Ersdal, L. Imsland, and K. Uhlen, "Model predictive load-frequency control," *IEEE Trans. on Power Systems*, vol. 31, no. 1, pp. 777–785, Jan 2016.
[27] B. Gao, G. K. Morison, and P. Kundur, "Voltage stability evaluation using modal analysis," *IEEE Trans. on Power Systems*, vol. 7, no. 4, pp. 1529–1542, Nov 1992.
[28] G. K. Morison, B. Gao, and P. Kundur, "Voltage stability analysis using static and dynamic approaches," *IEEE Trans. on Power Systems*, vol. 8, no. 3, pp. 1159–1171, Aug 1993.
[29] F. Milano, *Power System Modelling and Scripting*. London: Springer, 2010.
[30] T. H. Sikiru, A. A. Jimoh, and J. T. Agee, "Inherent structural characteristic indices of power system networks," *Int. J. of Elec. Power & Energy Systems*, vol. 47, pp. 218–224, 2013.
[31] G. Yesuratnam and D. Thukaram, "Congestion management in open access based on relative electrical distances using voltage stability criteria," *Electric Power Systems Research*, vol. 77, no. 12, pp. 1608–1618, 2007.
[32] I. K. Dassios, P. Cuffe, and A. Keane, "Visualizing voltage relationships using the unity row summation and real valued properties of the flg matrix," *Electric Power Systems Research*, vol. 140, pp. 611–618, 2016.
[33] Illinois Center for a Smarter Electric Grid (ICSEG), "IEEE 39-Bus System," URL: http://publish.illinois.edu/smartergrid/ieee-39-bus-system/.
[34] F. Milano, "A Python-based software tool for power system analysis," in *Procs of the IEEE PES General Meeting*, Vancouver, BC, pp. 1–5, July 2013.
[35] A. Stankovic, M. Ilic, and D. Maratukulam, "Recent results in secondary voltage control of power systems," *IEEE Trans. on Power Systems*, vol. 6, no. 1, pp. 94–101, Feb 1991.
[36] H. Mehrjerdi, S. Lefebvre, M. Saad, and D. Asber, "A decentralized control of partitioned power networks for voltage regulation and prevention against disturbance propagation," *IEEE Trans. on Power Systems*, vol. 28, no. 2, pp. 1461–1469, May 2013.

Álvaro Ortega (S'14, M'16) received the degree in Industrial Eng. from Escuela Superior de Ingenieros Industriales, Univ. of Castilla-La Mancha, Ciudad Real, Spain, in 2013. In 2017, he received the Ph.D. in Electrical Eng. from Univ. College Dublin, Ireland, where he is currently a senior power systems researcher. His research interests include dynamic modelling and control of energy storage systems, and transient and frequency stability analysis of power systems.

Federico Milano (S'02, M'04, SM'09, F'16) received from the Univ. of Genoa, Italy, the ME and Ph.D. in Electrical Eng. in 1999 and 2003, respectively. From 2001 to 2002 he was with the Univ. of Waterloo, Canada. From 2003 to 2013, he was with the Univ. of Castilla-La Mancha, Spain. In 2013, he joined the Univ. College Dublin, Ireland, where he is currently Professor of Power System Control and Protections and Head of Electrical Engineering. His research interests include power system modeling, stability analysis and control.